Plastic Deformation of Crystalline Polymers: The Role of Cavitation and Crystal Plasticity

Andrzej Pawlak and Andrzej Galeski*

Centre of Molecular and Macromolecular Studies, Polish Academy of Sciences, Sienkiewicza 112, 90-363 Lodz, Poland

Received April 20, 2005; Revised Manuscript Received August 3, 2005

ABSTRACT: Plane strain compression in a channel die is kinematically very similar to drawing; however, the possibility of void formation is limited due to a compressive component of stress. In drawing, voids were detected by small-angle X-ray scattering (SAXS) and density measurements in poly(methylene oxide) (POM), polypropylene (PP), and high-density polyethylene (HDPE), but no voiding was found in polyamide 6 (PA 6), low-density polyethylenes (LDPEs), and ethylene−octene copolymer (EOC). The slope and shape of the initial elastic part of true stress−true strain curves are similar in tension and in channel die compression. When drawn samples of POM, PP, HDPE, and PA 6 already show yielding, the channel die compressed samples still undergo elastic deformation to a much larger deformation and respond with a much larger stress. Channel die compressed POM, PP, HDPE, and PA 6 exhibit strong and rapid strain hardening up to 400 MPa in contrast to their behavior in tension. The difference in strain hardening is related to preservation of chain entanglement density in channel die compression and disentanglement in tensile drawing. True stress−true strain curves for polymers having crystals with low plastic resistance and not cavitating are very similar in channel die compression and in tension. In tensile drawing there is a competition between cavitation and activation of crystal plasticity. Cavitation occurs in polymers with crystals of higher plastic resistance, while plastic deformation of crystals in polymers with crystals of lower plastic resistance. The necessary conditions for cavitation and for plastic deformation of crystal are defined. They explain why the cavitation is observed in POM, PP, and HDPE but not in LDPEs. In PA 6 negative pressure causes cavitation but the cavities, due to their small sizes and healing action of surface tension, are unstable, close quickly, but leave the traces of a structural damage. A model of plastic deformation of crystalline polymers accounting for cavitation is outlined.

Introduction

Plastic deformation mechanisms of crystalline polymers play a crucial role in their mechanical performance. Recently, three reviews showing different aspects of plastic deformation were published;[1−3] however, the understanding of processes undergoing on a submicron scale is still incomplete. Nearly all information about plastic deformation is based on tensile type of tests, with analysis of the necking conditions, arrangement of molecules, and rearrangement of crystallites in the neck.[4−9] Much less attention was paid to the studies of plastic deformation of polymers under compression[10,11] or shear.[12,13] The main mechanisms of plastic deformation observable on a microscopic scale for amorphous polymers are crazing and shear yielding. It is thought that in crystalline polymers above their glass transition temperature the yield is determined by the stress required for the plastic deformation of crystals. The knowledge of plastic deformation of crystalline phase is rather well established, with attention given to such aspects as crystallographic slips, rearrangement of the lamellae structure, and role of the defects of crystalline structure.[14−18] However, the role of cavitation in plastic deformation of crystalline polymers has not been completely clarified to this time. The possibility of cavitation under external force strongly depends on the character of applied deformation and is larger under tension than under compression. Cavitation on the macroscale is visible as whitening. The voiding was observed in many drawn polymeric materials such as polypropylene[19−22] and high-density polyethylene,[23] but not in some others like ethylene−α-olefin copolymer.[4,5] It was established in the past that a low crystallinity level and a fine spherulitic structure are advantageous for development of crazes in semicrystalline polymers.[24] Unlike in amorphous polymers crazing in semicrystalline polymers is not restricted to temperatures below T_g but occurs also above the glass transition of the amorphous phase.[25] Below T_g long crazes propagate perpendicularly to load direction ignoring internal polymer structure while at a temperature close to T_g crazes are confined to several spherulites.[26,27] Radicals formed due to the chain scission of macromolecules were observed in oriented polymers during tensile deformation.[28,29]

The internal cavitation observed in tension experiments has been referred to as "micronecking" by Peterlin.[30] It was supposed that "micronecking" removes kinematic constraints between lamellae and allow them to untangle. However, from this picture as imagined by Peterlin, it follows that the drawing of crystalline polymers inherently involves cavitation as an essential feature. While the above picture is reasonable in tensile deformation, it is not correct for the modes of deformation not producing cavitation, in which positive pressure component prevents formation of cavities. "Micronecking" is inessential for the development of nearly perfect single-crystal textures, as was shown for several semicrystalline polymers that result from the deformation modes involving a positive pressure component.[31−35] One of the possibilities of cavity-free deformation is by plane strain compression in a channel die.[36] Plane strain compression in a channel die is kinematically very similar to drawing: the sample is extended, and its cross

* Corresponding author. E-mail: andgal@bilbo.cbmm.lodz.pl.

10.1021/ma050842o CCC: $30.25
Published on Web 10/22/2005

Table 1. Characteristics of Polymers Studied

polymer	molecular mass M_w	M_w/M_n	MFI [g/10 min] (2.16 kg, 190 °C)	density [g/cm^3]	comments
POM Tarnoform 300 (Tarnow, Poland)			9.0	1.410	copolymerization of trioxan with dioxolan
PA6 Capron 8200, (Allied Chem.)	3.2×10^4	1.8		1.130	extracted
PP Novolen 1100L (BASF)	3.1×10^5	5.0	5.0 (at 230°C)	0.910	injection grade
HDPE Lupolen 6021D (BASF)	1.8×10^5	7. 2	0.26	0.960	blow molding grade
EOC Exact 0203 (Dex Plastomers, Netherlands)	7.6×10^4	2.68	3.0	0.902	ethylene based octene plastomer (copolymer)
LDPE Lupolen 1840D (BASF)	4.5×10^5		0.25	0.919	film grade
LDPE Lupolen 2420H (BASF)	3.0×10^5		2.1	0.924	film grade
LDPE Malen E FGAN 18-D003 (Orlen, Poland)			0.2	0.921	film grade

section decreases accordingly. However, no neck is formed, and the possibility of voids formation is limited due to a compressive component of stress. It is reasonable to expect that similar elementary plastic deformation mechanisms are initiated under similar true stress in tension and in plane strain compression. It means that any differences in true stress−true strain dependences of drawn and plane strained materials should be attributed to the formation and development of cavities. The number of observations of polymer deformation behavior under positive pressure at the level preventing cavitation which can be found in the literature[37] is limited, and no comparison with tensile drawing was made. The aim of these studies is to show differences in the mechanical responses of several semicrystalline polymers in extensional deformation with and without cavitation. Special attention was paid to the formation of voids and to their influence on plastic deformation.

Useful experimental configuration for the studies of material properties under plane strain compression is the so-called channel-die system.[36,38] In the channel die apparatus, because of the presence of side constrains, the sample has the possibility to deform freely only in one direction, called a flow direction. The plane-strain deformation in the channel die configuration is kinematically quite similar to uniaxial tension, and the results of both tests can be compared. When comparing the results of experiments, a number of factors need to be taken into account. These include the similarity of true strain rates and whether the experiments have been performed in tension or in compression, i.e., considering the tension−compression asymmetry. With regard to the latter, one should account for the differences in the elastic part of true stress−true strain dependence in tension and in compression, while above this region one may use the measurements of Bartczak et al.[43] that demonstrated that polymer crystal yielding obeyed the Coulomb law where the shear resistance is dependent on the normal stress acting across the glide plane.

Comparison of the material response for the two different loading procedures, drawing and plane strain compression, may supply the information about internal mechanisms of plastic deformation, especially about the role of cavitation, which should not be present when a positive pressure component is involved.

Experimental Section

Materials. The following crystallizing polymers were selected for the studies: poly(methylene oxide), POM (Tarnoform 300, Zaklady Azotowe Tarnow, Poland), polyamide 6, PA6 (Capron 8200, Allied Chem.), isotactic polypropylene, PP (Novolen 1100L, BASF), ethylene−octene copolymer, EOC (Exact 0203, DSM/Exxon Mobil Chem., Dex Plastomers, Netherlands), high-density polyethylene, HDPE (Lupolen 6021D, BASF), and three branches of low-density polyethylenes LDPE: Lupolen 2420H (BASF), Lupolen 1840D (BASF), and Malen E FGAN (Orlen, Poland). The characteristics of materials used in the studies, based on the producers and our own data, are collected in Table 1. Samples of all materials, with the exception of polyamide, were injection-molded, using a Battenfeld 30 g injection molding machine. The temperatures of the barrel were 185 °C for EOC and HDPE, 190 °C for POM and all LDPEs, and 195 °C for PP. The temperature of the mold was 20 °C. The shape of samples was according to ASTM D638M-93 standard with 10 mm width and 4 mm thickness.

POM before injection was dried for 1.5 h at 100 °C. The mold was with wide entrance, and the injection of all polymers was performed at a low injection speed in order to avoid the orientation effect as much as possible. The skin layer was characterized by mostly perpendicular orientation of lamellae with respect to flow direction for all polymers tested as was determined by SEM examination of etched cross sections of the samples (permanganic etchant for polyolefins, formic acid for POM and PA6). The preferred lamellae orientation was limited to 100−150 μm thick layer in all injection-molded samples. One of the means to determine the skin effect on crystallinity is to measure the difference in melting enthalpies and melting temperature between the core and skin of the samples. They were for POM 166.4 J/g vs 156.9 J/g and 165.9 °C vs 164.8 °C, for HDPE 194.6 J/g vs 184.1 J/g and 134.9 °C vs 133.3 °C, and for PP 100.6 J/g vs 95.2 J/g and 164.2 °C vs 164.2 °C for the core and for the skin, respectively. As is seen from these data, the skin effect on crystallinity is relatively small in all tested samples.

Polyamide 6 was prepared by compression-molding, after drying. The samples of PA 6 for studies were cut from 3.2 mm thick sheets to the standard shape removing the skin, and surfaces of cutting were polished.

The samples for channel die compression tests were cut out to the size of 15 × 6 × 3.5−3.8 mm from injected pieces. Their surfaces were machined and polished in order to remove any surface flaws and reduce friction against the channel die walls.

Methods. Tensile tests were performed on an Instron 5582 tensile testing machine. Injection-molded samples were used for drawing after 48 h aging since the injection. Tensile tests were conducted at the room temperature of 23 °C. To preserve a constant strain rate, the speed of the Instron machine crosshead was controlled by the strain gauge placed in the necking area of a sample. A momentary strain rate of 5%/min was maintained for the entire drawing experiment.

In addition, the actual three dimensions of a deformed sample in the necking area were recorded by a video camera and used later for the precise determination of true strain and for calculations of true stresses. Five samples of each material were tested.

A channel die, the description of which was given in detail elsewhere[39] and briefly presented in Figure 1, was used for performing plane strain compression. Our channel die was similar in design to that used by Gray and Young;[40] however, its dimensions were changed to minimize friction: 15 mm wide, 4 mm high, and only 6 mm long, and the walls were polished. The contribution of friction to measured stress was

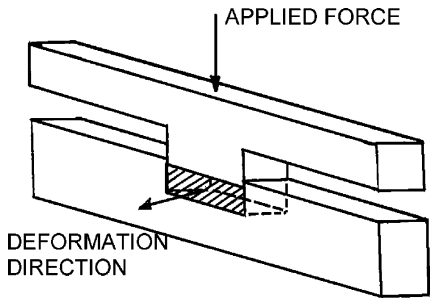

Figure 1. Arrangement of channel die for plane strain compression of polymer samples.

evaluated by comparing two channel die compression tests of the HDPE sample: one without a lubricant and one with silicon oil lubrication. It was found that for this newly designed channel die at the stress level of 400 MPa (at the true strain of 2.08) the effect of lubrication was within the scatter of results for unlubricated HDPE samples; hence, no additional lubrication was applied for channel die compression. The temperature of the channel die was maintained at 23 °C, similarly as for the tensile tests. The device was located inside the working area of an Instron machine which was used for applying a controlled load. Two parameters—force and true strain, determined by an extensometer—were measured. The load was applied in a controlled way to ensure a constant momentary deformation rate along the channel at the same level of 5%/min as in tensile drawing. The increment of strain in x-direction was equal to $-\Delta h/h$ in a channel die having the length L and increment of strain in tensile drawing was equal to $\Delta l/l$, where h and l were the momentary height and length of the samples, respectively. The quantities $-\Delta h/h$ and $\Delta l/l$ were controlled and kept constant during tensile and channel die experiments in consecutive time intervals.

The true strain in the case of channel die compression was defined as $e = \int_h^{h_0}(\mathrm{d}u/u) = \ln(\mathrm{CR})$, h being the momentary height of the sample, h_0 being the initial height of the sample, and CR being the compression ratio while in tension $e = \int_{l_0}^{l}(\mathrm{d}u/u) = \ln(l/l_0)$, where l is the momentary length of a chosen section of the sample, l_0 is the initial length of a chosen section, and l/l_0 is the local strain.

The small-angle X-ray scattering technique (SAXS) was used for measuring the long period and for the detection of voids. A 1.1 m long Kiessig-type camera was equipped with a pinhole collimator and an imaging plate as a recording medium (Kodak). The camera was coupled to a X-ray generator (sealed-tube, fine point Cu Kα filtered source operating at 50 kV and 35 mA, Philips PW 1830), equipped with a capillary collimator (X-ray Optical Systems Inc.) enabling the resolution of scattering objects up to 60 nm. The scattered radiation was recorded using imaging plates. Exposed imaging plates were read with a PhosphorImager SI system (Molecular Dynamics). The scattered intensity after Lorentzian correction was a base for the long period determination. Also the correlation function was calculated according to the procedure described by Goderis et al.[41]

Thermal properties were measured using a differential scanning calorimeter DSC 2920 (TA Instruments). The 7−8 mg samples were heated from ambient temperature at the rate of 10 deg/min. A nitrogen atmosphere was maintained in the chamber during the test.

The densities of polyolefin samples were determined by the flotation method using mixtures of ethanol and water, while for PA6 the mixture of CCl_4 + heptane and for POM the aqueous solution of $ZnCl_2$ was used. Measurements were performed at room temperature after 1 h conditioning of a sample inside the flotation mixture.

Results

Mechanical Response of Materials to Tension and Plane Strain Compression. The mechanics of compression in a channel die needs some comments. Let us examine a rodlike sample with rectangular cross section under external tensile load and a similar sample in the channel die under external load applied by a plunger. This portion of calculations, which follow, is limited to the elastic range only.

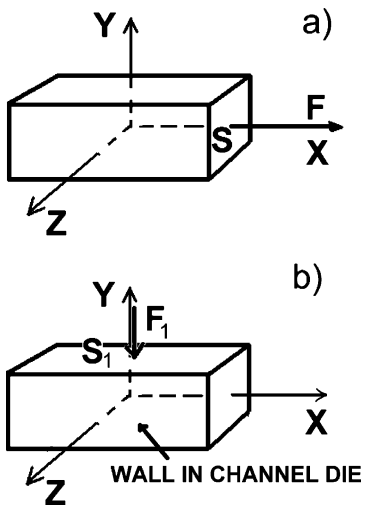

Figure 2. Scheme of forces acting during the tests: (a) tensile drawing, (b) compression.

The scheme of forces acting in drawing and in channel die compression is presented in Figure 2a,b. For channel die configuration the elasticity equations are as follows:

$$\epsilon_x = \frac{1}{E}(-\nu(\sigma_{ym} + \sigma_z)) = -\frac{\nu(1+\nu)}{E}\sigma_{ym} \tag{1a}$$

$$\epsilon_y = \frac{1}{E}(\sigma_{ym} - \nu\sigma_z) = \frac{\sigma_{ym}}{E}(1-\nu^2) \tag{1b}$$

$$\epsilon_z = -\frac{\nu\sigma_{ym}}{E} + \frac{\sigma_z}{E} = 0 \tag{1c}$$

where ν is the Poisson coefficient and E is the modulus of elasticity. Here $\sigma_{ym} = F_1/S_1$ and σ_z is the stress representing the reaction of walls.

In the x-direction there are two free ends giving $\sigma_x = 0$ while in the z-direction there are two perpendicular walls, which prohibit the deformation in this direction, so $\epsilon_z = 0$. There are two parameters measured during the channel die experiment: σ_{ym} and ϵ_y. From the above equations it follows that the acting stress inside the material is

$$\sigma_y = (1-\nu^2)\sigma_{ym} \tag{2}$$

This correction for the stress must be introduced into the true stress−true strain curves from channel die data and then used for characterization of elastic properties and for comparison with tensile data.

Inside the plastic region it is expected that the Coulomb criterion[42] should be applied for crystal deformation. It was demonstrated[43] that polymer crystal yielding obeys the Coulomb law where shear resistance τ is dependent on normal stress σ_n acting across the glide plane according to the relation

$$\tau = \tau_0 - K\sigma_n \tag{3}$$

where τ_0 is the plastic resistance of a crystal in simple shear and K is the stress sensitivity factor. The value

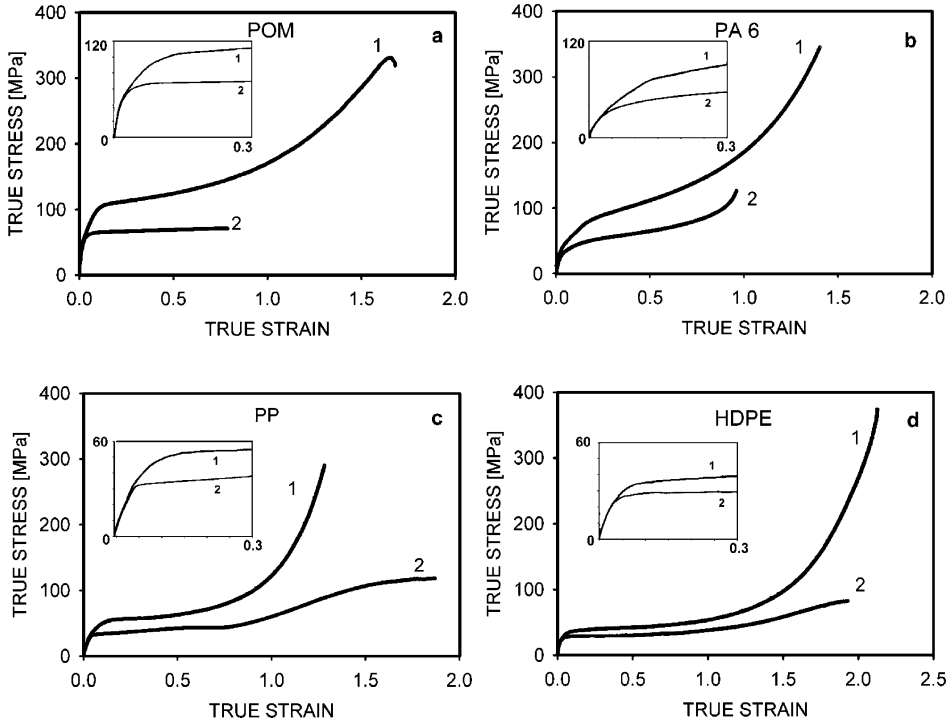

Figure 3. True stress−true strain curves for several polymers: (a) poly(methylene oxide), (b) polyamide 6, (c) polypropylene, (d) high-density polyethylene. Curves 1 represent typical properties of the material during channel die compression; curves 2 represent tensile experiments. The true stress values in channel die compression were compensated according to the correction derived in the text.

of stress sensitivity factor, K, for many polymer crystals is usually of the order of 0.1.[43]

Simple calculations show that flow stress σ_{yield} in compression should be equal to

$$\sigma_{yield} = 2\tau_0/(1 + K) \quad (4a)$$

due to the easiest slip system activated at 45° while in tension, it should be

$$\sigma_{yield} = 2\tau_0/(1 - K) \quad (4b)$$

for the same reason. Therefore, the difference between stresses in compression and in tension for the yield and plastic flow should be around 20% for $K = 0.1$.

The above reasoning indicates that the mechanical response of the sample in tension and in channel die should be very similar. The difference is in 3D stress, i.e., the pressure: for tensile experiments the pressure $p = -\sigma_x/3$ has always a negative value because σ_x is positive, while in the channel die pressure $p = -(\sigma_{ym} + \sigma_z)/3$ has always positive values because σ_{ym} and σ_z are negative. For polymeric materials yielding typically at the stress of tens of MPa, the pressure does not reach high values; e.g., for a polymer showing yield at 30 MPa the pressure at yield is −10 MPa in tensile experiments, while +15 MPa in a channel die compression.

Assuming that the deformation involves similar micromechanisms during plane strain compression and tension, the corresponding true stress−true strain curves corrected for the elastic region according to eq 2 should be similar.

The yield and plastic flow on true stress−true strain curves, corrected for stress sensitivity factor K as followed from Coulomb criterion, should appear at similar stress and strain levels in the tensile and plane strain compression experiments if the same mechanisms of plastic deformation of crystals are activated. The disagreement between experimental data for these two ways of plastic deformation may indicate the activity of other mechanisms of deformation.

Experimental True Stress−True Strain Curves. The response of four crystalline polymers POM, PA 6, PP, and HDPE during compression in a channel die and in drawing is shown in Figure 3. This group of polymers is characterized by rather high values of elastic modulus and high yield stress which are used for stiffness and strength requiring products.

The presented true stress−true strain curves (corrected for the elastic region according to eq 2 assuming Poisson ratio of 0.3 for POM,[44] 0.33 for PA6,[45] 0.35 for PP,[46] 0.46 for HDPE,[47] and corrected by stress sensitivity factor K, as followed from the Coulomb criterion, for the remaining fragment of the curves) represent a typical response to the deformation applied during drawing and during channel die compression. The slope and shape of the initial elastic part of curves are similar in tension and in channel die compression within an experimental error (see insets in Figure 3). This is a good test for the correctness of the applied procedure. The similarity of the initial elastic part of true stress−true strain curves indicates that those curves can be directly compared. Although all these polymers, POM, PA 6, PP, and HDPE, were able to deform plastically, the differences begin to be seen with the onset of plastic yielding in drawing (see the insets in Figure 3, yield stress and yield strain are determined as stress and strain where the two tangents to the initial and final parts of the true stress−true strain curve intersect).

The most intriguing difference occurs for the samples compressed in a channel die: when drawn samples already show yielding, the channel die compressed samples still undergo elastic deformation to a much larger true strain and respond with a much larger true

Table 2. Yield Stress of Crystalline Polymers in Channel Die Compression and in Tension, Corrected for Stress Sensitivity Factor *K* as Followed from the Coulomb Criterion, Yield Strain, and Elastic Moduli Corrected According to Eq 2

	compression			tension		
polymer	corrected yield stress [MPa]	yield strain	Young modulus [MPa]	corrected yield stress [MPa]	yield strain	Young modulus [MPa]
POM	95.4	0.07	3170	69.3	0.04	3190
PA6	63.0	0.09	1980	46.2	0.04	2000
PP	49.6	0.09	1360	34.1	0.05	1350
HDPE	31.5	0.06	1050	25.3	0.04	1030
EOC	5.4	0.07	210	5.5	0.06	215
LDPE Lupolen 1840D	8.1	0.07	195	7.7	0.06	190
LDPE Lupolen 2420H	9.0	0.06	250	9.9	0.05	250
LDPE Malen E	9.9	0.07	195	8.8	0.05	205

stress, as is seen in Figure 3. The yield stresses and strains for all these polymers are significantly larger in channel die compression than in tensile experiments, as evidenced in Table 2 where the yield stresses of crystalline polymers studied in channel die compression and in tension, corrected for stress sensitivity factor *K* as followed from the Coulomb criterion, and true strains at yield are listed. The differences depend on the category of a polymer. The largest differences are for poly(methylene oxide) for which the yield stress corrected for stress sensitivity factor *K* as followed from the Coulomb criterion for the channel die compressed sample is much larger than that for tensile test (95.4 MPa vs 69.3 MPa, see Table 2). A similar scale of difference is observed for PA 6, for which the corrected yield stress for channel die compressed samples is 63.0 and 46.2 MPa for drawn material. The true strain at yield for channel die compressed materials are in the range of 0.06−0.09 while for drawn samples 0.04−0.06 only. The differences in corrected yield stress for POM, PA6, PP, and HDPE are so large that they cannot be explained by plastic deformation of crystals alone.

Another striking difference in the mechanical response of crystalline polymers deformed in the channel die and in tension is their behavior at larger strains. Channel die compressed polymers resist large true stresses, up to 400 MPa, i.e., to the limit of our Instron machine, for all polymers presented in Figure 3, and most of them do not fracture at that stress. The same materials tested in tension hardly show strength above 100 MPa and often brake at a much lower strain (POM and PA 6). All channel die compressed samples exhibit strong and rapid strain hardening in contrast to their behavior in tension. Apparently, the plastic flow and the activation of strain hardening are initiated in a different way or involve different mechanisms.

The other group of polymers, which is characterized by low elastic modulus and low yield stress and used for the production of soft flexible films and packaging, chosen for this study, consists of various low-density polyethylenes and an ethylene−octene copolymer. Their mechanical behavior in the form of true stress−true strain curves is presented in Figure 4. The presented true stress−true strain curves were corrected for the elastic region according to eq 2 assuming the Poisson ratio for LDPE and EOC of 0.45.[48]

Similarly, as for the group of stiff and strong polymers from Figure 3, the initial slope (see Table 2) and shape

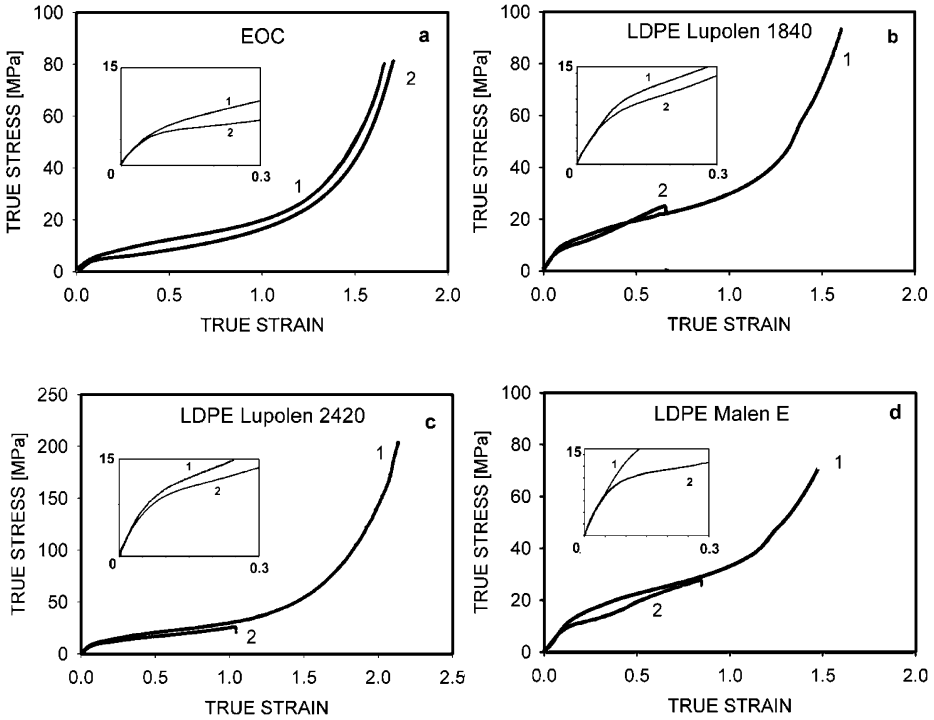

Figure 4. True stress−true strain curves for several polymers: (a) EOC Exact, (b) LDPE Lupolen 1840, (c) LDPE Lupolen 2420, (d) LDPE Malen E. Curves 1 represent typical properties of material during channel die compression; curves 2 represent tensile experiments. The true stress values in channel die compression were compensated according to the correction derived in the text.

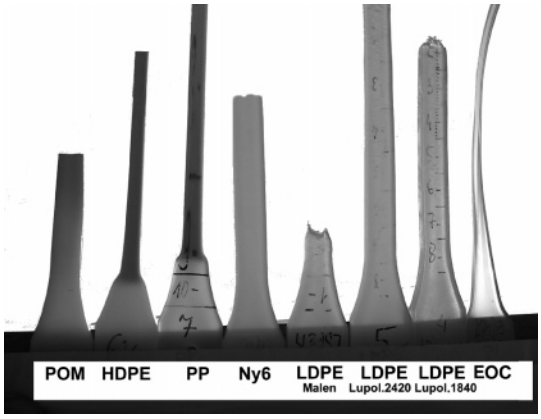

Figure 5. Comparison of transparency of drawn samples. From left to right: POM, HDPE, PP, PA 6, LDPE Malen E, LDPE Lupolen 2420, LDPE Lupolen 1840, EOC.

(see the insets in Figure 4) of the true stress−true strain curves are very similar in channel die compression and in tension. In contrast to strong and stiff polymers from the first group, the yield of soft polymers is reached in channel die compression and in tension at a similar corrected true stress and at a similar true strain (see Table 2). Parts of the true stress−true strain curves beyond yield are also very similar for both deformation modes, indicating similar acting mechanisms of plastic flow.

The true strains at break for those tensile samples are in the range of 0.7−1.7, being smaller than in the compressed samples, for which they were in the range of 1.4−2.1. However, the mechanisms involved in fracture of crystalline polymers are different than those exhibited in their plastic deformation. Cross-sectional and surface instabilities, which operate in tensile experiments rather than in channel die compression, may lead to a premature fracture in tension.

Observation of Cavitation. A visible sign of cavitation during deformation of a polymer is its significant whitening. A comparison of transparency of drawn samples of the polymers studied is presented in Figure 5. The regions with large plastic deformation and undeformed ends of samples are shown. Intense whitening due to plastic deformation occurs in drawing for POM, PP, and HDPE but not for PA 6, EOC, and all LDPEs (Lupolen 1840, Lupolen 2420, and Malen E). In contrast to the drawn samples, all channel die compressed polymers showed no whitening and became progressively more transparent when compressed to a higher compression ratio, irrespective of a polymer type.

The cavitation influences the density of the deformed material. The densities of materials are presented in Table 3. For LDPEs and EOC the differences in densities before and after deformation are insignificant, within the range of the accuracy of measurements (0.005 g/cm^3).

For other polymers a decrease in density was observed for drawn samples: poly(methylene oxide) (4%), polypropylene (5%), and HDPE (9%). Only 1% decrease of density was recorded for drawn polyamide 6.

No differences of densities were recorded for channel die compressed samples, with the exception of PP, for which the density decreased from 0.909 to 0.895 g/cm^3. However, the entire decrease of the density of PP can be attributed to a decrease in its crystallinity which occurred during channel die compression as it follows from the decrease of enthalpy of melting from 100.6 to 85.2 J/g (see Table 4). In other polymers the crystallinity also changes due to deformation, but the changes are diverse and rather small.

The crystallinity increases slightly due to drawing for LDPEs of initial density of 0.917 g/cm^3 and ethylene−octene copolymer where the effect is similar to orientational crystallization of rubber.

Similar behavior was also observed earlier in PP and PA 6 where the crystallinity increases slightly due to drawing.[49,50] In HDPE the crystallinity decreased slightly due to channel die compression as found earlier.[51,52]

Changes in the internal structure caused by deformation can be detected in SAXS patterns. The scattering from voids is much more intense than from periodic amorphous−crystalline stacks due to much larger density difference. The voids are easily detected in SAXS scattering images if their size is in the range from 2 to 60 nm.

The selected SAXS scattering images obtained from POM, PA 6, PP, and HDPE samples drawn to increasing true strains are presented in Figure 6. The direction of

Table 3. Density Changes in Tested Materials

polymer	initial density [g/cm^3]	true strain in drawing	density after tensile test [g/cm^3]	true strain in channel die compression	density after compression [g/cm^3]
POM	1.407	0.8	1.361	1.7	1.402
PA6	1.143	0.9	1.136	1.4	1.137
PP	0.909	1.8	0.861	1.2	0.895
HDPE	0.957	1.9	0.872	2.0	0.949
EOC	0.905	1.7	0.910	1.4	0.905
LDPE Lupolen 1840D	0.917	0.7	0.918	1.6	0.916
LDPE Lupolen 2420H	0.921	1.0	0.922	2.0	0.922
LDPE Malen E	0.921	0.8	0.922	1.5	0.920

Table 4. Thermal Properties of Oriented Samples Studied by DSC

	enthalpy of melting [J/g]			temperature of melting [°C]		
	initial	stretched	compressed	initial	stretched	compressed
POM	166.4	166.6	167.2	165.9	166.7	167.0
PA6	67.2	71.0	67.9	222.6	223.5	223.0
PP	100.6	105.5	85.2	164.2	164.7	165.4
HDPE	194.6	199.2	189.9	134.9	137.8	137.5
EOC	90.1	93.8	96.5	99.7	99.8	99.8
LDPE Lupolen 1840D	110.0	116.6	109.0	108.8	109.4	109.6
LDPE Lupolen 2420H	122.8	123.4	126.1	112.4	113.4	112.8
LDPE Malen E	126.9	122.6	129.6	111.2	112.4	113.5

Table 5. Surface Tensions[62−64] and Negative Pressures Involved in Cavitation during Drawing

polymer	surface tension [mJ/m^2]	amorphous layer thickness[a] [nm]	negative press. needed to maintain cavity open [MPa]	tensile yield stress, σ_{yield} [MPa]	negative press. generated at yield around newly formed cavities [MPa]
POM	44.6	4.69	−35.8	63	−42.0
PA6	38.4	5.59	−33.6	42	−28.0
PP	29.4	8.16	−13.7	31	−20.7
HDPE	35.7	9.45	−15.1	23	−15.3
LDPEs	35.3	7.50	−17.6	7	−4.7

[a] Calculated on the basis of SAXS long period and DSC degree of crystallinity.

deformation is horizontal, and the true strain was chosen from 0.1 in small increments up to 1.8 or to true strain just before fracture. For POM, PP, and HDPE the sudden appearance of a large fraction of voids is detected at low true strain of 0.1. No scattering by voids was detected for PA 6 at any true strain. For HDPE voiding is detected at low and intermediate true strains. For higher true strain the scattering in SAXS pattern disappears, suggesting that the voids are either larger than the resolution of the SAXS camera or have disappeared. The results of density measurements (Table 3) suggest that in the drawn or compressed PA 6 no voids are present, while in the drawn HDPE there is the largest fraction of voids among the polymers studied. Apparently, voids in the HDPE drawn to high true strain are larger in either direction than the upper resolution of the SAXS camera used.

The short axis of voids can be calculated from the profile of scattered intensity based on the Grubb and Prasad[53] and Wu[54] approach. Calculations give 22 nm for the short void axis in highly drawn PP, 31 nm for POM, and 40 nm for HDPE (true strain 1.1). In drawn POM, PP, and HDPE initially the voids are slightly elongated along the direction perpendicular to drawing and mimic the dilatational crazing. In PP the voids become reoriented with longer axis along the drawing direction at the true strain of 0.2 and higher, while for POM and HDPE the voids do not change their orientation as the true strain increases.

2D SAXS patterns for channel die compressed POM, PA 6, HDPE, and PP do not indicate any voiding. No voiding was found by SAXS measurements for LDPEs and EOC in drawing and in channel die compression.

It is reasonable to assume that the physics of cavitation occurring in the amorphous phase during deformation of crystalline polymers is similar to cavitation in a molten fraction of a polymer during its crystallization: it requires the generation of a negative pressure at a similar level of −3.5 to −20 MPa (HDPE from −3.5 to −10 MPa,[55] PP from −13 to −19 MPa,[56−58] POM from −10 to −18 MPa[56−58]).

It is known that the stress in heterogeneous systems is not homogeneously distributed. On sites with a misfit of mechanical properties the stress concentrates; its value may increase locally manyfold and trigger cavitation. In the case of crystalline polymers such sites are between differently oriented packets of lamellae, and the stress concentration factor can reach 3 or more.

In the paper by Galeski, Argon, and Cohen,[59] the imprints of cavitation were revealed by osmium tetroxide staining in drawn PA 6, Capron 8200—the same material and the same samples which were used in these studies. The cavitation occurred in the amorphous layers confined by the crystalline lamellae. In fact, the cavities left traces of damaged material having the size of the order of the interlamellar distance, i.e., 4−5 nm.

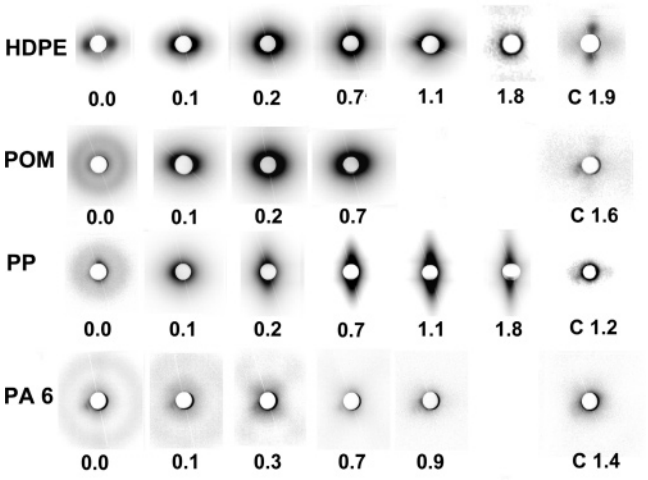

Figure 6. 2-D SAXS patterns for undeformed and deformed samples. Direction of drawing and flow direction in the case of channel die compression are horizontal. From left to right: undeformed polymer, after drawing (different local true strains) and after channel die compression (C). True strains are shown below respective SAXS patterns.

Since cavitational voids are having sizes on the nanoscale level, there is a problem of their stability. On each nanopore the surface tension is exerted from the very beginning of its formation, which tends to close a pore. To preserve a pore, the action of a negative pressure is required at the level which is reciprocally proportional to the pore radius:

$$p = -2\gamma_s/r \tag{5}$$

where γ_s is the surface tension and r is the size of a pore. It follows then that the smallest pores are healed readily, while larger ones can be preserved only if the negative pressure is maintained at a sufficiently high level. The lack of negative pressure or its inadequate level will lead to a spontaneous healing of cavitational pores; otherwise, they can grow in the course of drawing.

In the paper by Muratoglu et al.[60] it was shown that when cavitational pores arise they form initially spherical voids (which later grow and become elongated). It is then logical to suppose that at the moment of cavity formation the stress concentrates around spherical inhomogeneity and, as was calculated by Goodier[61] for spherical inclusions, is increased by the factor of 2. Also, the negative pressure generated is increased accordingly.

In Table 5 the data on surface tension, thickness of the amorphous layers, negative pressure needed to maintain the cavity open (according to eq 5 assuming the radius of newly formed cavity equal to half of the amorphous layer thickness), and the yield stress in drawing are presented. In the last column of Table 5 the negative pressure generated at yield around newly

Table 6. Parameters of Nondeformed Materials Determined by SAXS and DSC

polymer	long period from SAXS intensities [nm]	long period from correlation function [nm]	peak melting temperature [°C]	crystallinity from DSC [%]
POM	14.2	13.0	165.9	67
PA 6	8.0	7.6	222.6	35
PP	15.4	14.0	164.2	47
HDPE	27.8	25.8	134.9	66
EOC	12.2	12.0	99.7	29
LDPE Lupolen 1840D	12.4	11.4	108.8	37
LDPE Lupolen 2420H	12.4	10.6	112.4	42
LDPE Malen E	13.2	12.0	111.2	43

formed cavities is listed. These values of pressure result from the stress at yield ($-\sigma_{yield}/3$) increased by the factor of 2 arising from the stress concentration as predicted by Goodier.[61]

It is clearly seen that the negative pressure at concentration sites, which is the negative pressure at yield ($-\sigma_{yield}/3$) multiplied by stress concentration factor 3, can cause cavitation in the case of PA 6, POM, PP, and HDPE because it is higher than the negative pressure for cavitation in polymer melts (HDPE from −3.5 to −10 MPa,[55] PP from −13 to −19 MPa,[56−58] POM from −10 to −18 MPa[56−58]), but not adequate for cavitation of LDPEs.

In POM, PP, and HDPE the yield stress generates sufficient negative pressure around cavities to maintain them and to boost their further growth. In fact, the cavitation in those polymers during drawing is evidenced by density decrease (Table 3) and strong small-angle X-ray scattering (Figure 6). However, it is also evident that the negative pressure generated around newly formed cavities is not sufficient to keep them open in the case of PA 6; the cavities in PA 6 are unstable and will heal quickly. Actually, the transmission electron microscopy (TEM) examination[59] of the same material does not expose any empty voids but only traces of chemically changed material between crystalline lamellae. It should be mentioned here that the growth of cavities proceeds in fact due to the deformation of the surrounding matter; therefore, it is due to the action of deviatoric stresses and not due to negative pressure.

Competition between Cavitation and Crystal Plasticity. The data on initial lamellae thickness and crystallinity of the materials studied, based on SAXS and DSC measurements, are collected in Table 6. There is a large spectrum of long period values from 8.0 nm for PA 6 to 27.8 nm for HDPE. The values based on the determination of the correlation function from SAXS data are slightly lower but consistent with those determined from peak intensity (Lorentz corrected) vs scattering vector curves. Also, the crystallinities are different: from 29 to 43% for ethylene−octene copolymer and low-density polyethylenes through 35% for PA 6 to 66−67% for HDPE and POM. Comparison of these data with mechanical properties leads to the conclusion that polymers with higher crystallinity and thicker long period, e.g., POM, PP, and HDPE are those for which large differences in tensile and plane strain compression responses are visible. The exception from this scheme is PA 6, which is not very crystalline having a small long period, but characterized by high melting temperature. It suggests that its crystals are rather strong, exhibiting high resistance to shear. In fact, polyamide 6 exhibits high critical shear stress for crystallographic slips.[35]

From Table 6 it is evident that the differences in tension/channel die compression tests were the largest in those polymers in which the crystals were more rigid and resistant to plastic deformation, such as in POM, PA 6, PP, and HDPE. The level of stress necessary to achieve plastic deformation of crystals in the second group of materials is much smaller than in the first group. Negative pressure generated at concentration sites under such stress is then lower than the negative pressure needed to cause cavitation (below −20 MPa). In compression, the yield stress reflects the plastic resistance of crystals.

There are clear dependencies describing the activation of either cavitation or crystal plasticity: the cavitation during drawing can be observed only in polymers in which stress σ generates a negative pressure higher than that required for cavitation.

$$\sigma/3 = -p > -p_{cav} \tag{6a}$$

where p is the negative pressure generated and p_{cav} is the negative pressure required for cavitation. If we account for the stress concentration between lamellae, where cavitation preferably occurs, then the stress concentration factor may be as high as 3 or more and the pressure, p, is increased accordingly.

In the other case a crystallographic slip will occur earlier relaxing the stress, and cavitational pores will not appear. This necessary condition for the activation of crystallographic slips can be written in the form

$$\sigma > 2\tau_0/(1 - K) \tag{6b}$$

From the above condition it follows that cavitation during drawing can be expected in such polymers as nylons (the easiest slip for PA 6 is at $\tau_0 = 16.24$ MPa[35]), polypropylene ((010)[001] slip at around $\tau_0 = 22-25$ MPa[17,65]), poly(methylene oxide)[66] because the negative pressure for cavitation in those polymers is at the level of 10−19 MPa only. If thick crystals are present, cavitation can be observed in polyethylene, since only thick PE crystals exhibit high enough plastic resistance.[67−69] No cavitation is expected during deformation of low-density polyethylene and quenched high-density polyethylene, both having usually thin lamellar crystals, but cavitation can be found in HDPE which is slowly cooled when forming thick wall products.

It follows that in drawing there is a competition between cavitation and activation of crystal plasticity: easier phenomena occur first, cavitation in polymers with crystals of higher plastic resistance, and plastic deformation of crystals in polymers with crystals of lower plastic resistance.

Strain Hardening. Beyond the yield in all channel die compressed polymers from Figure 3 a short region of plastic flow is followed by a strong strain hardening. In drawing (Figure 3), the plastic flow region is longer and strain hardening is slight (PA 6, PP, and HDPE) or even not pronounced before fracture (POM).

In polymers strain hardening is known to originate from straightening of the network of entanglements. In drawing there are evidences from the recovery experiments[6,70] that a significant chain untangling takes place. Evidently, in channel die compression the chain disentanglement is strongly limited.

In the paper by Schoenherr, Vancso, and Argon[71] concerning the AFM studies of channel die compressed HDPE deformed to the compression ratio of 6.44 (the sample from the work of Galeski et al.[31]), a molecular resolution in AFM images was achieved. The molecular resolution reached in their studies revealed no clearly identifiable amorphous layers over several expected long period dimensions, confirming the dispersion of the amorphous material and the diffusion of previously clear amorphous−crystalline interface. Careful scrutiny of those micrographs, however, revealed a collection of well-dispersed chain defects in the form of flip-overs of two parallel chains and other ill-defined short-range irregularities among the well-aligned macromolecules. These defects can be identified as entanglement knots which were carried along with lamellae fragments at high compression ratio and incorporated into newly formed crystals. The number of entanglement knots which can be counted from a series of four AFM micrographs from the paper by Schoenherr et al.[71] gives the average chain fragment between entanglement knots at the level of $M_w = 1350$ (66 knots visible in four micrographs of the (100) crystallographic plane areas of 10 nm × 10 nm). An earlier estimate based on the rheological studies of polyethylene melt gives the average molecular weight of a chain fragment between two entanglement knots of 1200−1300.[72−74] An important conclusion can be drawn from the fact that these two values are very close: no significant disentanglement takes place during plastic deformation of polyethylene up to the high strain, provided that there is no cavitation. A similar result is expected for other polymers based on the observation of strong strain hardening in plane strain compression.

Conclusions

Plane strain compression in a channel die is kinematically very similar to drawing: the sample is extended, and its cross section decreases accordingly. However, the possibility of void formation is limited due to the compressive component of stress. It means that the differences in true stress−true strain dependencies of drawn and plane strained polymers should be attributed to the formation and development of cavities. Slopes of the elastic region of true stress−true strain curves are similar in tension and plane strain compression. The difference in mechanical properties of polymers sets in at yielding in tension. The scale of difference depends on a particular polymer: the yield in drawing for POM, PA 6, PP, and HDPE takes place at a much lower stress than in plane strain compression. For polymers with low crystal plastic resistance, LDPEs and EOC, the stresses at a selected deformation ratio were very similar for both modes of sample loading. The conclusion is that the cavitation during deformation can be observed only in those polymers in which the value of negative pressure generated at yield is higher than the value of negative pressure required for cavitation. Otherwise, the crystals will deform earlier relaxing the stress and cavitation will not appear.

Beyond the yield in channel die compressed POM, PA 6, PP, and HDPE, a short region of plastic flow is followed by a strong strain hardening, while in drawing the plastic flow region is longer and strain hardening is only slightly pronounced before fracture. Nearly no difference in plastic flow and strain hardening is observed for soft LDPEs and EOC in drawing and plane strain compression.

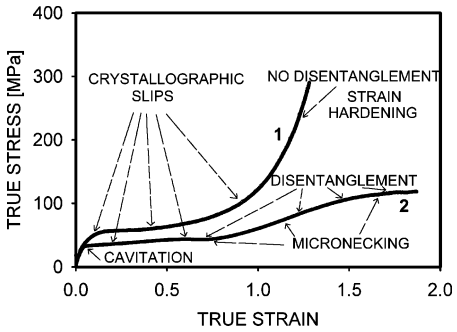

Figure 7. Mechanisms associated with plastic deformation of crystalline polymers explained on the example of isotactic polypropylene: curve 1, channel die compression; curve 2, tensile experiment.

SAXS, densitometry, and TEM[59] show a clear correlation of the formation of cavities in tension with a decrease of the yield stress when compared to the yield stress without cavitation (plane strain compression). It is also evident that cavitation is the reason for low strain hardening and intense chain disentanglement during drawing with cavitation. In turn, no significant disentanglement takes place during plastic deformation of polymers up to a high strain, provided that there is no cavitation.

Mechanisms associated with plastic deformation of crystalline polymers can be explained better on the basis of two examples of isotactic polypropylene subjected to drawing and to plane strain compression in a channel die. The envisioned differences between deformation with and without cavitation are summarized in Figure 7.

The initial part of the elastic region of true stress−true strain curves is common for drawing and for plane strain compression. As the strain increases, the material starts to yield in drawing at the stress level which is usually considered as the yield stress of a particular polymer and placed in product information sheets. However, the stress level at yield corresponds rather to the onset of cavitation and not necessarily to the onset of plastic deformation of crystals. With the progress of drawing, the cavitational pores extend in the direction of drawing and the polymeric material between them starts to deform plastically, including now crystal plasticity mechanisms, giving rise to the long known "micronecking" phenomena and leading for large drawing ratios to a "microfibrillar" morphology. Along with cavitation and micronecking the chain disentanglement takes place, promoted by the formation of a large fraction of new free surfaces of voids. The chain disentanglement becomes intense; it results in loosening of the entanglement network and limits significantly the strain hardening.

In plane strain compression, the elastic region extends to a larger strain and larger stress because the formation of cavitation is not in operation, while crystal plasticity needs higher resolved shear stresses to become active. When the stress reaches the level sufficient for triggering the easiest crystallographic slip (for example of iPP as in Figure 7 (100)[001] chain slip system at

the critical resolved shear stress of 22.6 MPa,[17] also 25 MPa[65]), crystal plasticity overtakes the control of further deformation process. The real yield stress for polypropylene from Figure 7, as determined by crystal plasticity, is now at the level of 50−55 MPa.

In plane strain compression the plastic flow ends shortly and strain hardening induced by straightening of the entanglement network sets in. Since no or little chain disentanglement occurs, the stress reaches very high values at a relatively low true strain.

Acknowledgment. Grant KBN 7T08E 055 22 from the State Committee for Scientific Research Poland is acknowledged for the financial support of the work.

References and Notes

(1) Galeski, A. *Prog. Polym. Sci.* **2003**, *28*, 1643−1699.
(2) Argon, A. S.; Cohen, R. E. *Polymer* **2003**, *44*, 6013−6032.
(3) Oleinik, E. F. *Polym. Sci., Ser. C* **2003**, *45*, 17−117.
(4) Butler, M. F.; Donald, A. M.; Ryan, A. J. *Polymer* **1997**, *38*, 5521−5538.
(5) Butler, M. F.; Donald, A. M.; Ryan, A. J. *Polymer* **1998**, *39*, 39−52.
(6) Hiss, R.; Hobeika, S.; Lynn, C.; Strobl, G. *Macromolecules* **1999**, *32*, 4390−4403.
(7) Popli, R.; Mandelkern, L. *J. Polym. Sci., Polym. Phys. Ed.* **1987**, *24*, 441−483.
(8) Juska, T.; Harrison, I. R. *Polym. Eng. Rev.* **1982**, *22*, 766−776.
(9) Gent, A. N.; Madan, S. *J. Polym. Sci., Polym. Phys. Ed.* **1989**, *27*, 1529−1542.
(10) Bartczak, Z.; Cohen, R. E.; Argon, A. S. *Macromolecules* **1992**, *25*, 4692−4704.
(11) Lee, B. J.; Argon, A. S.; Parks, D. M.; Ahzi, S.; Bartczak, Z. *Polymer* **1993**, *34*, 3555−3575.
(12) Castelein, G.; Coulon, G.; G'Sell, C. *Polym. Eng. Sci.* **1997**, *37*, 1694−1701.
(13) Aboulfaraj, M.; G'Sell, C.; Ulrich, B.; Dahoun, A. *Polymer* **1995**, *36*, 731−742.
(14) Crist, B. *Polym. Commun.* **1989**, *30*, 69−71.
(15) Young, R. J. *Mater. Forum* **1988**, *11*, 210−216.
(16) Lin, L.; Argon, A. S. *J. Mater. Sci.* **1994**, *29*, 294−323.
(17) Bartczak, Z.; Galeski, A. *Polymer* **1999**, *40*, 3677−3684.
(18) Haudin, J. M. In *Plastic Deformation of Amorphous and Semicrystalline Materials;* Escaig, B., G'Sell, C., Eds.; Les Editions de Physique: Paris, 1982; p 291.
(19) Duffo, P.; Monasse, B.; Haudin, J. M.; G'Sell, C.; Dahoun, A. *J. Mater. Sci.* **1995**, *30*, 701−711.
(20) Li, J. X.; Cheung, W. L. *Polymer* **1998**, *39*, 6935−6940.
(21) Li, J. X.; Cheung, W. L.; Chan, C. M. *Polymer* **1999**, *40*, 2089−2102.
(22) Li, J. X.; Cheung, W. L.; Chan, C. M. *Polymer* **1999**, *40*, 3641−3656.
(23) Piorkowska, E.; Galeski, A.; Kryszewski, M. *Colloid Polym. Sci.* **1982**, *260*, 735−741.
(24) Keith, H. D.; Padden, F. J., Jr. *J. Appl. Phys.* **1964**, *35*, 1270.
(25) Kausch, H. H.; Gensler, R.; Grein, Ch.; Plummer, J. G.; Scaramuzzino, P. *J. Macromol. Sci., Phys.* **1999**, *B38*, 803−815.
(26) Friedrich, K. *Adv. Polym. Sci.* **1983**, *52/53*, 225−274.
(27) Narisawa, I.; Ishikawa, M. *Adv. Polym. Sci.* **1990**, *91/92*, 353.
(28) Kausch, H. H. *J. Macromol. Sci., Rev. Macromol. Chem.* **1970**, *C4*, 243−280.
(29) Crist, B.; Peterlin, A. *Makromol. Chem.* **1973**, *171*, 211−227.
(30) Peterlin, A. In *Polymeric Materials;* Baer, E., Ed.; American Society for Metals: Metals Park, OH, 1975; pp 175−195.
(31) Galeski, A.; Bartczak, Z.; Argon, A. S.; Cohen, R. E. *Macromolecules* **1992,** *25*, 5705−5718.
(32) Pluta, M.; Bartczak, Z.; Galeski, A. *Polymer* **2000**, *41*, 2271−2288.
(33) Bellare, A.; Cohen, R. E.; Argon, A. S. *Polymer* **1993**, *34*, 1393−1403.
(34) Boontongkong, Y.; Cohen, R. E.; Spector, M.; Bellare, A. *Polymer* **1998**, *39*, 6391−6400.
(35) Lin, L.; Argon, A. S. *Macromolecules* **1994**, *25*, 4011−4024.
(36) Galeski, A.; Argon, A. S.; Cohen, R. E. *Macromolecules* **1991**, *24*, 3953−3961.
(37) Kapur, S.; Matsushige, K.; Galeski, A.; Baer, E. In *Advances in Research on Strength and Fracture of Materials*; Taplin, D. N. R., Ed.; Pergamon Press: New York, 1978; pp 1079−1086.
(38) Bartczak, Z.; Cohen, R. E.; Argon, A. S. *Macromolecules* **1992**, *25*, 4692−4704.
(39) Bartczak, Z. In *Deformation, Yield and Fracture of Polymers—12th International Conference;* IOM Communications: London, 2003; pp 416−418. Also: Bartczak, Z. *Polymer* **2005**, *46*, 10339−10354.
(40) Gray, R. W.; Young, R. J. *J. Mater. Sci.* **1974**, *9*, 521−522.
(41) Goderis, B.; Reynaers, H.; Koch, M. H. J.; Mathot, V. B. F. *J. Polym. Sci., Part B: Polym. Phys.* **1999**, *37*, 1715−1738.
(42) Ward, I. M.; Hadley, D. W. *An Introduction to the Mechanical Properties of Solid Polymers.*; Wiley: New York, 1993; pp 213−231.
(43) Bartczak, Z.; Argon, A. S.; Cohen, R. E. *Macromolecules* **1992**, *25*, 5036−5053.
(44) Lesser, A. J. *Polym. Eng. Sci.* **1996**, *36*, 2366−2374.
(45) *Polymer Handbook*, 4th ed.; Brandrup, J., Immergut, E. H., Grulke, E. A., Eds.; Wiley: New York, 1999; p V/128.
(46) Jancar, J. In *Handbook of Polypropylene and Polypropylene Composites*; Karian, H. G., Ed.; Marcel Dekker: New York, 1999.
(47) Data on Poisson ratio of HDPE from Goodfellow Co., London, U.K. (www.Goodfellow.com).
(48) *Encyclopedia of Polymer Science and Engineering*; Wiley: New York, 1986; Vol. 5, p 370.
(49) Kalinski, R.; Galeski, A.; Kryszewski, M. *J. Appl. Polym. Sci.* **1981**, *26*, 4047−4058.
(50) Kowalewski, T.; Kalinski, R.; Galeski, A.; Kryszewski, M. *Colloid Polym. Sci.* **1982**, *260*, 652−662.
(51) Bartczak, Z.; Galeski, A.; Argon, A. S.; Cohen, R. E. *Polymer* **1996**, *37*, 2113-2123.
(52) Bartczak, Z.; Morawiec, J.; Galeski, A. *J. Appl. Polym. Sci.* **2002**, *86*, 1405−1412.
(53) Grubb, T.; Prasad, K. *Macromolecules* **1992**, *25*, 4575−4582.
(54) Wu, J. *Polymer* **2003**, *44*, 8033−8040.
(55) Piorkowska, E.; Galeski, A. *J. Polym. Sci., Part B: Polym. Phys.* **1993**, *31*, 1285−91.
(56) Pawlak, A.; Piorkowska, E. *J. Appl. Polym. Sci.* **1999**, *74*, 1380−1385.
(57) Nowacki, R.; Kolasinska, J.; Piorkowska, E. *J. Appl. Polym. Sci.* **2001**, *79*, 2439−2448.
(58) Galeski, A.; Piorkowska, E. In *Liquids Under Negative Pressure;* NATO Sci. Ser., II. Mathematics, Physics and Chemistry, Vol. 84; Imre, A. R., Maris, H. J., Williams, P. R., Eds.; Kluwer Academic Publisher: Dordrecht, 2002; pp 127−136.
(59) Galeski, A.; Argon, A. S.; Cohen, R. E. *Macromolecules* **1988**, *21*, 2761−2770.
(60) Muratoglu, O. K.; Argon, A. S.; Cohen, R. E.; Weinberg, M. *Polymer* **1995**, *36*, 4771−4786. *Polymer* **1995**, *36*, 4787−4795.
(61) Goodier, J. *Trans. ASME* **1933**, *55*, 39−42.
(62) Wu, S. *Polymer Interface and Adhesion;* Marcel Dekker: New York, 1982; pp 88−92.
(63) Kasemura, T.; Yamashita, N.; Suzuki, K.; Kondo, T.; Hata, T. *Kobunshi Ronbunshu* **1978**, *35*, 263.
(64) *Polymer Handbook,* 4th ed.; Brandrup, J., Immergut, E. H., Grulke, E. A., Eds.; Wiley: New York, 1999.
(65) Shinozaki, D.; Groves, G. W. *J. Mater. Sci.* **1973**, *8*, 71−78.
(66) Kaito, A.; Nakayama, K.; Kanetsuna, H. *J. Appl. Polym. Sci.* **1986**, *32*, 3499−3513.
(67) Kazmierczak, T.; Galeski, A. In *Proceedings of VIth ESAFORM Conference on Material Forming*; Univ. Salerno, Italy, 2003.
(68) Kazmierczak, T.; Galeski, A. In *Proceedings of 12th International Conference on Deformation, Yield and Fracture of Polymers,* Cambridge, UK, Apr 7−10, 2003.
(69) Brooks, N. W. J.; Mukhtar, M. *Polymer* **2000**, *41*, 1475−1480.
(70) Al-Hussein, M.; Strobl, G. *Macromolecules* **2002**, *35*, 8515−8520.
(71) Schoenherr, H.; Vancso, G. J.; Argon, A. S. *Polymer* **1995**, *36*, 2115−2121.
(72) Raju, V. R.; Smith, G. G.; Martin, G.; Knox, J. R.; Graessley, W. W. *J. Polym. Sci., Polym. Phys. Ed.* **1979**, *17*, 1183−1195.
(73) Cassagnau, P.; Montfort, J. P.; Martin, G.; Monge, P. *Rheol. Acta* **1993**, *32*, 156−167.
(74) Gell, C. B.; Graessley, W. W.; Fetters, L. J. *J. Polym. Sci., Part B: Polym. Phys.* **1997**, *35*, 1933−1942.

MA050842O